Is "metamictization" of zircon a phase transition?

E.K.H. SALJE,[1,]* J. CHROSCH,[1] AND R.C. EWING[2]

[1]Department of Earth Sciences, University of Cambridge, Downing Street, Cambridge CB2 3EQ
[2]Department of Nuclear Engineering and Radiological Sciences and Department of Geological Sciences, The University of Michigan, Ann Arbor, Michigan 48109-2104, U.S.A.

ABSTRACT

Diffuse X-ray scattering from single crystals of metamict zircon reveals residual crystallinity even at high fluences (up to 7.2×10^{18} α-decay events/g). The experimental evidence does not suggest that radiation-induced amorphization is a "phase transition." The observations are in good agreement with a nonconvergent, heterogeneous model of amorphization in which damage production is a random process of cascade formation and overlap at increasing fluence.

Instead of an amorphization transition, the existence of a percolation transition is postulated. At the level of radiation damage near the percolation point, the heterogeneous strain broadening of X-ray diffraction profiles is reduced whereas the particle-size broadening increases. Simultaneously, the macroscopic swelling of the zircon becomes larger than the maximum expansion of the unit-cell parameters. A suitable empirical parameter that characterizes this transition is the flux, D_s, at which the macroscopic expansion is identical to the maximum expansion of the crystallographic unit cell. In zircon, $D_s = 3.5 \cdot 10^{18}$ α-decay events/g.

INTRODUCTION

"Metamictization" is the transition from the crystalline to an aperiodic or amorphous state due to alpha-decay event damage from constituent radionuclides (^{238}U, ^{235}U, and ^{232}Th) and their daughters (Ewing 1994). However, this transformation in minerals is part of a larger class of radiation-induced transformations to the amorphous state that has received considerable recent attention as a result of ion- and electron-beam experiments on metals (Johnson 1988), intermetallics (Motta 1996; Motta and Olander 1990), simple oxides (Gong et al. 1996a, 1996b; Degueldre and Paratte 1998), and complex ceramics and minerals (Wang and Ewing 1992; Ewing et al. 1987, 1995; Weber et al. 1998; Wang and Weber 1998). Different models have been proposed in which radiation-induced amorphization is either a homogeneous process caused by defect concentrations reaching a critical value (Okamoto and Meshii 1988; Fecht and Johnson 1988; Wolf et al. 1990; Lam and Okamoto 1994a, 1994b) or a heterogeneous process caused by cascade "quenching" and overlap with increasing dose (Meldrum et al. 1998; Wang et al. 1998a, 1998b). Most previous workers have implicitly assumed that metamictization is a "driven" phase transition with a well-defined critical dose that varies as a function of temperature (Weber et al. 1994; Meldrum et al. 1997). Such critical doses are commonly determined as the dose at which there is a loss of crystallinity as revealed by the absence of an X-ray or electron diffraction maximum. Such a definition is clearly unsatisfactory, particularly for standard X-ray diffraction experiments, as the sensitivity with which X-ray signals may be detected depends strongly on experimental details. In fact, we observe clear X-ray diffraction signals at the position of Bragg reflections from all samples which were previously characterized as fully amorphous. The diffraction intensity disappear asymptotically with increasing radiation dose and it makes no sense to define a physical parameter by that dose at which no diffraction is observed under some "standard" but ill-defined experimental condition. Furthermore, glasses may show a characteristic diffraction pattern, $S(Q)$, with diffraction maxima close to those of related crystal structures. Such a glassy material with local order can be confused with samples that contain small areas of undamaged material in an aperiodic matrix. It is also important to quantify the dose-dependence of the radiation damage as a function of physical and structural properties. In many previous experimental studies, the damage was measured by macroscopic density changes and unit-cell expansion (Holland and Gottfried 1955; Murakami et al. 1991). Macroscopic swelling often follows an empirical dose dependence of the type (Weber 1993)

$$\Delta V_m/V_0 = A_m [1 - \exp -(B_m D)^n] \tag{1}$$

where D is the dose, A_m is the saturation swelling, B_m is a constant related to the mass of material damaged per decay event, and n is an empirical exponent with typical numerical values between 1 and 2.5. Note that this model contains no critical dose. The saturation swelling is approached asymptotically, and no phase transition is considered on a macroscopic length-scale.

On an atomic-scale level, radiation damage accumulation has been successfully modeled based on the idea that a periodic array of atoms is disrupted if each atom is displaced at least three times by a radiation-induced displacement cascades; this defines the double-overlap model (Gibbons 1972). In this model, direct amorphization does not occur in any single cascade, but rather a

---

*E-mail: es10002@esc.cam.ac.uk

catastrophic collapse of local structure occurs at a critical defect concentration. Accordingly, the volume fraction of amorphous material depends on the dose according to:

$$f_a = 1 - [(1 + B_d D + B_d^2 D^2 / 2) \exp(-B_d D)] \qquad (2)$$

where B_d is the total mass of material damaged per alpha-decay event. Good agreement between experiment and the predicted dose dependence of f_a has been found for zircon (Murakami et al. 1991; Weber 1993). The double overlap model implies a critical dose, only, in so far as it assumes that the local structure collapses only if a critical defect concentration is reached. The in-cascade amorphization is not considered to be the important process because the damaged regions develop randomly. The macroscopic amorphous state is approached exponentially in this model, which precludes the definition of a critical dose beyond which the sample becomes "fully" amorphous.

Another common approach for the description of radiation damage in crystals is based on the concept of a "driven phase transition" (DPT). DPTs were originally postulated for the behavior of metallic alloys under radiation. The fundamental idea is that the role of entropy in thermodynamic phase transitions is taken over by the process of randomization of atomic positions by ballistic events. In such ballistic events the incoming particles (e.g., α-particles) knock atoms out of their lattice site and "drive" the system toward a state of a higher degree of disorder. This state is then similar to (but not identical with) a high-temperature phase in which entropy was generated thermodynamically. Thus, the concept of DPTs tries to rescue much of the theories of structural phase transitions in thermodynamic equilibrium and apply them with slight modifications to a typical non-equilibrium situation (Martin and Bellon 1997).

For DPTs, the thermal transition between the disordered and the ordered state should be reduced in temperature by the radiation damage. Furthermore, a continuous transition tends to become discontinuous if the ballistic events become more important. Although this treatment is appealing by its simplicity, there is no experimental evidence in zircon or other silicates that supports this approach. In fact, the idea of driven phase transitions is closely related to the inverse temperature hypothesis (e.g., Wagner 1952), which provides a direct connection between ballistic and thermal jumps. The validity of this hypothesis was questioned by Tsatskis and Salje (1988).

So far we have argued that the concept of a critical dose for complete amorphization of zircon is unphysical and that there is no indication of a DPT to take place. We now turn to the question whether a macroscopic "phase transition" with the radiation dose as control parameter is conceptually meaningful. Let us assume that the crystal structure can fully relax after each radiation event. We can then derive an expression for the energy density of the crystal as follows.

In a simple energy expression related to the swelling of a volume element for $f_a > 0$, we may define the excess volume as the shrinking of the specific (e.g., molar) volume V with respect to the fully amorphous reference state ($f_a = 1$). From

$$\Delta V = V_{periodic} - V_{aperiodic} < 0 \qquad (3)$$

the energy gain due to crystallization may be formulated as the combination of four effects:

(1) the crystallization energy:

$$E_{matrix} = \mu \Delta V + \frac{1}{2} \mu' (\Delta V)^2 + ... \qquad (4)$$

(2) the energy related to the interaction between crystalline parts in an aperiodic matrix

$$E_{interaction} = \frac{1}{2} B (\Delta V)^2 + \frac{1}{4} C (\Delta V)^3 + ... \qquad (5)$$

and (3) the energy related to the interface between periodic and aperiodic parts of the sample (or any other variation of the local density).

$$E_{gradient} = \frac{1}{2} g (\text{grad } \Delta V)^2 + ... \qquad (6)$$

The parameters μ, μ', B, C, and g are constants related to the chemical potential, the volume enthalpies, and the gradient energies as often used in the field of structural phase transitions (e.g., Salje 1993). A further energy term relates to the interaction between the sample and the α-particles and/or the recoil nucleus damage process. If each "hit" produces an equal amount of damage, the collision energy E_{coll} is in lowest order

$$E_{coll} = AD\Delta V \qquad (7)$$

where A is a proportionality factor. If, on the other hand, the damage process is purely statistical, the collision energy depends on the probability for an undamaged part of the sample being "hit." In this case,

$$E_{coll} = -E_o [1 - \exp(-AD\Delta V)] \qquad (8)$$

where E_o is a scaling factor. The total energy (ignoring all thermal effects for this simple argument) is the sum of E_{matrix}, $E_{interacton}$, $E_{gradient}$, and E_{coll}. Minimizing this energy with respect of ΔV in the uniform case leads to

$$\mu + (\mu' + B) \Delta V + C (\Delta V)^2 - AD = 0 \qquad (9)$$

for collision of the type in Equation 7 while AD is replaced by $E_o \exp(-AD\Delta V)$ for statistical events of Equation 8. Ignoring C for small values of ΔV leads to a macroscopic transition with

$$\Delta V = -\frac{\mu - D}{\mu' + B}, \text{ or } \Delta V = 0 \qquad (10)$$

where D may be consider to be a control parameter. The volume decreases linearly as a function of dose, D, close to the transition point.

Alternatively, the purely statistical approach in Equation 8 leads to no phase transition for C = 0, i.e., the fully amorphous state is approached exponentially with no transition at all.

This simple model illustrates the crucial effect of the mechanism by which defects are generated. If overlapping cascades lead to amorphization, or if the probability for damage is greater in the crystalline parts of the sample than in the aperiodic parts, a phase transition is expected to occur. If the damage mechanism is purely statistical (ignoring thermal annealing effects, etc.) no such transition will occur. The dose dependence of the molar volume is in this case very similar to the temperature dependence of an order parameter in a "non-convergent" ordering process as discussed by Carpenter and Salje (1994 a, 1994b). We argue below that our experimental evidence for zircon is compatible with such behavior.

We can now identify two crucial questions, which need to be answered from the analysis of experimental observations:

(1) Is amorphization a process which leads to a phase transition (i.e., on a macroscopic scale)? (2) Do critical process occur on mesoscopic length scales?

It is the purpose of this paper to report new experimental evidence that shows that a very careful distinction between the radiation damage on a mesoscopic scale and on a macroscopic scale is necessary. We argue that locally amorphization is a critical process in which (quasi-) periodic regions either survive or collapse. Crudely speaking, this leads to a typical two-phase behavior with a phase mixture between periodic and aperiodic regions. The periodic regions collapse if their local defect density increases beyond a critical value or if their size decreases below a minimum. The implications for the statistical mechanics of the damage process are that we expect a percolation transition to exist but not a simple amorphization transition nor a DPT.

EXPERIMENTAL METHODS

Single crystals of zircon with various degrees of radiation damage were analyzed using X-ray diffraction techniques (Salje 1995; Locherer et al. 1996). Two types of experiments were performed. Each sample was analyzed using a full rocking geometry with three rocking circles and a 1200 position sensitive detector PSD(INEL) (Salje et al. 1993). In these experiments, diffraction maxima were identified, and the sample orientation was optimized with respect to the rocking angles ω and ψ (for definition of the angular settings see Salje 1995). The rocking curve was then measured with rotation angle omega and diffraction profiles measured in units of 2θ using PSD in the $\phi = 0$ position. The results were then displayed as intensity charts in the ω–θ plane. The widths of the maxima in either direction ω or θ were then calculated by curve fitting after the profiles were integrated along the θ or ω direction, respectively. Best fits were obtained for strongly metamict materials by Voigt profiles, similar to the procedure adopted by Murakami et al. (1991) for powder diffraction patterns.

In a second set of experiments, selected samples were analyzed using a 7-circle diffractometer (Salje 1995; Locherer et al. 1999). In this case, the detector was a two dimensional, planar wire detector with 10^6 pixels. For the diffraction experiment, all angles were optimized with the ω angle as rocking angle and Θ and χ as detector angles. Once the sample was aligned in diffraction position for Bragg peak (e.g., the 200 peak) the crystal was rotated by increments of $1/1000°$ around the rocking angle ω. For each angular step the diffraction intensities in a wide angular range (typically $\pm 10°$ in each direction) around the Bragg position was measured using the position sensitive detector (Fig. 1). In this way slices of diffraction intensities in reciprocal space were analyzed and combined numerically to construct a full three dimensional image of the diffraction profiles. All angles were transposed into reciprocal lattice space (h, k, l) and displayed with length scales in units of $1/Å$ (Locherer et al. 1996). The zircon samples were previously described by Murakami et al. (1991) and Ellsworth et al. (1994). Their compositions and radiation dose are summarized in Table 1.

TABLE 1. Summary of compositions and radiation dose

Sample	a (Å)	c (Å)	ρ (g/cm³)	Dose ($\times 10^{15}$ α/mg)
797	6.608(2)	5.980(2)	4.66	<0.05
4403	6.6085(2)	5.9845(3)	4.72	0.06(1)
3100			4.40(7)	4.0(1)
4304	6.67(1)	6.13(3)	4.36	5.8(3)
4105	6.70(1)	6.13(4)	4.35	6.3(3)
4103	6.70(4)	6.15(4)	4.17	6.7(3)
3107	≈6.7	≈6.2	4.12(1)	7.2(5)

FIGURE 1. Schematic view of the 7-circle diffractometer used for the measurement of diffuse diffraction signals in metamict samples. The sample is adjusted in the center of the cradle and rocked around the angles ϕ, χ, and ω to obtain the diffraction maximum in the middle of the position sensitive detector at the angle α. In subsequent experiments slices of diffraction space are measured as a function of the rocking angle ω and a full three-dimensional image of the diffraction profile in reciprocal space is derived numerically.
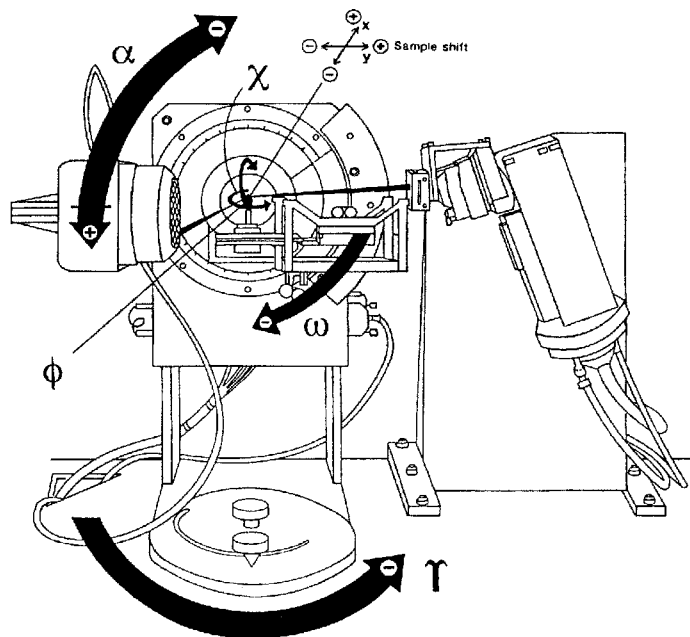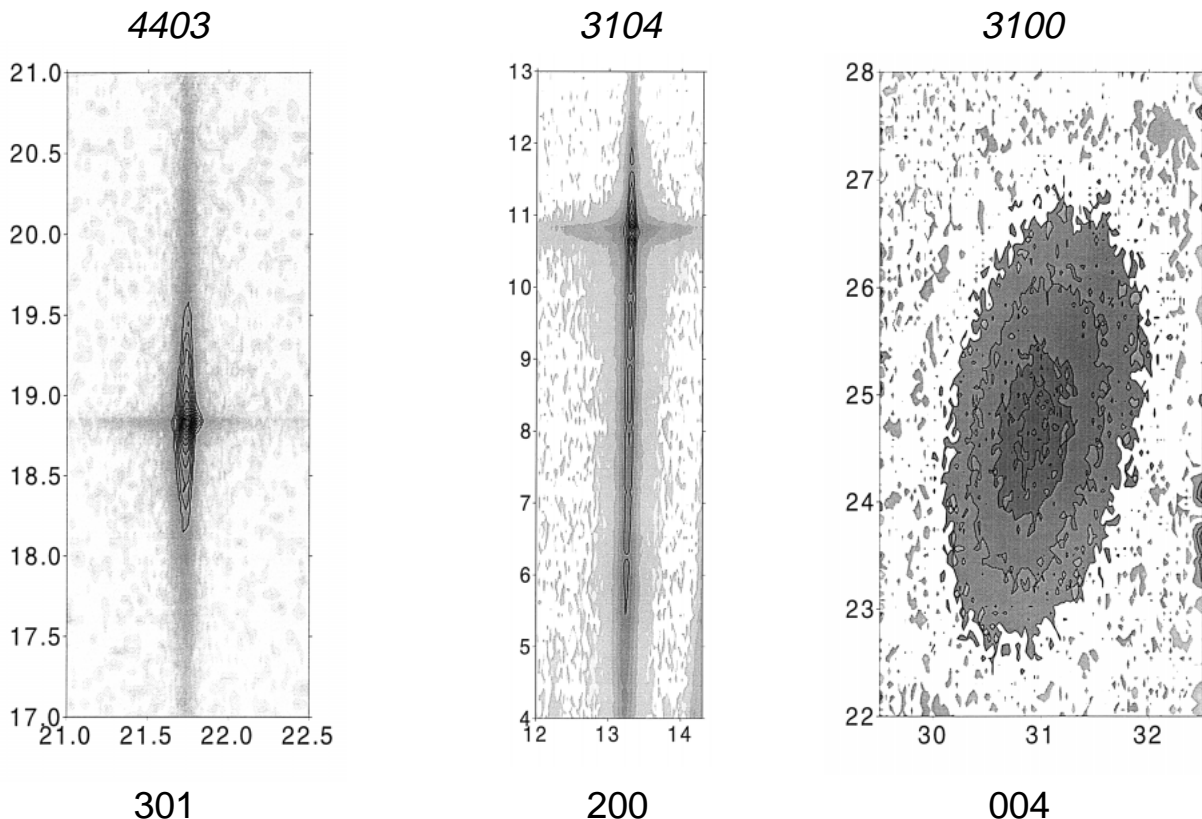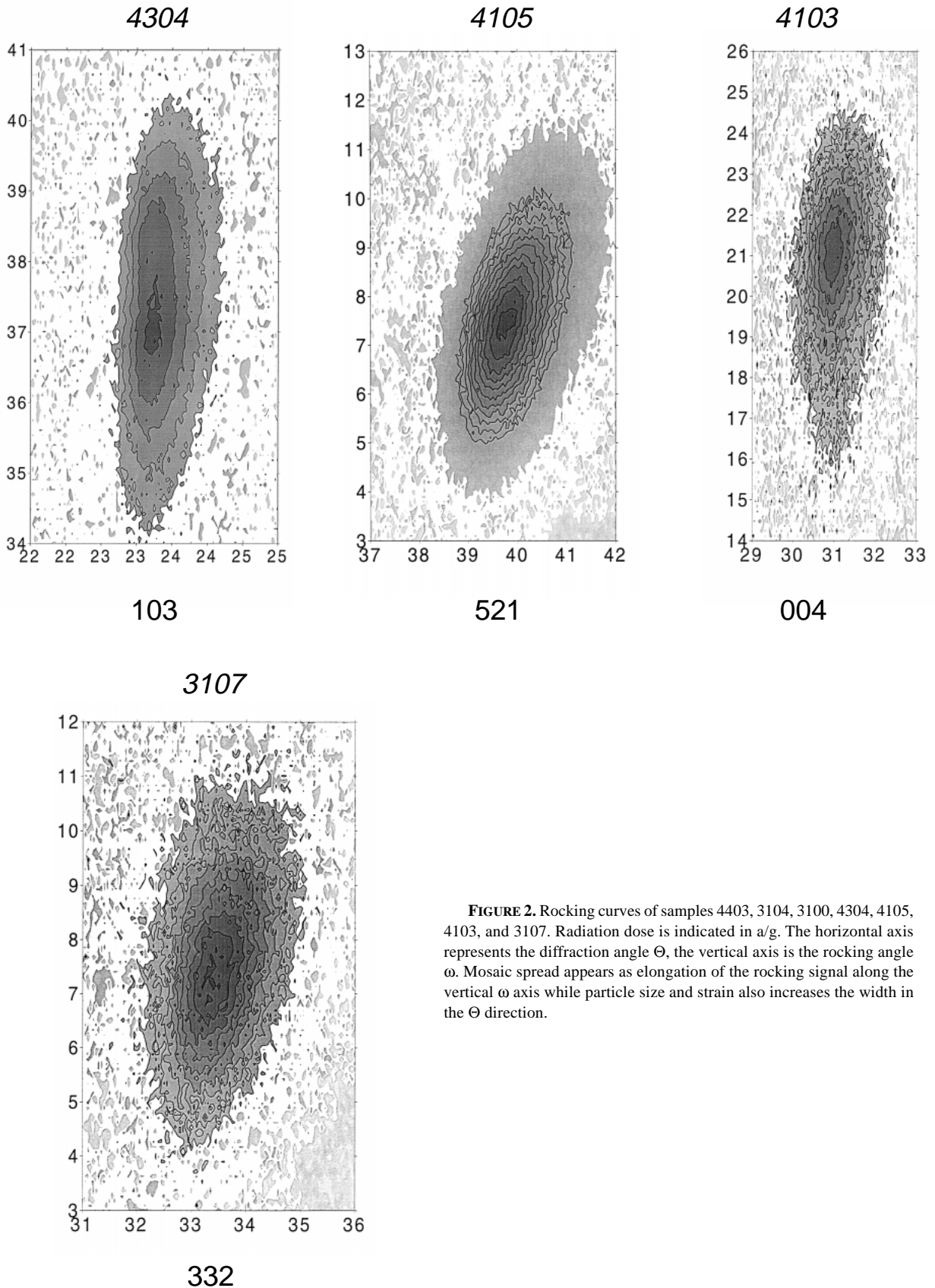
RESULTS

The two-dimensional rocking maps are shown in Figure 2. Well-defined Bragg peaks were found for all samples, including those with a radiation dose of $7.3 \cdot 10^{18}$ α-decay events/g that were previously thought to be fully amorphous (Stage III after Murakami et al. 1991). None of the samples shows sharp diffraction spots which are compatible with the experimental resolution of the experimental configurations (Chrosch and Salje 1996). All signals showed some strain and/or particle size broadening.
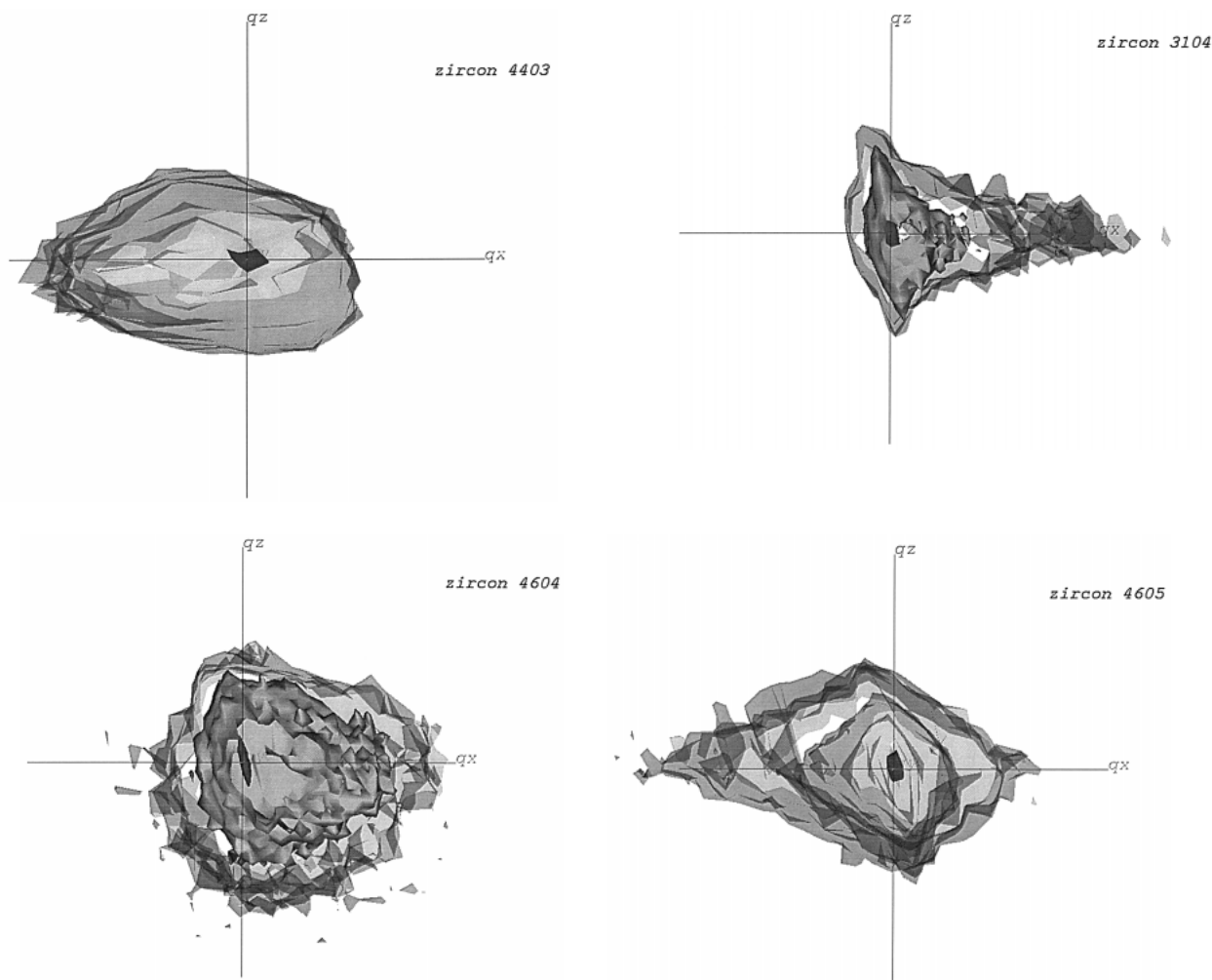
Bragg reflections are surrounded by halos of diffuse scattering. The centers of gravity of the halos are shifted with respect to the centers of the Bragg reflections. In the case of the lowest radiation dose, the shift is toward lower diffraction angles θ, while for all other samples the shift is toward higher diffraction angles. This observation agrees with earlier observations by Murakami et al. (1991) who used powder diffraction techniques. In addition to the diffuse scattering along the θ-direction, we find significant broadening along the ω direction. For low radiation doses the ω broadening is typical of mosaic crystals or crystals with rounded lattice planes. The mosaic spread is large (~2°) and increases weakly with increasing radiation dose. In samples with approximately $D > 4 \cdot 10^{18}$ α-decay events/g, the ω broadening is only slightly greater than the spread in the diffraction angle. This observation indicates that the diffuse scattering is dominated by particle size effects rather than by heterogeneous strain fields. The most surprising observation is that for no sample do we find sufficient ω spread to lead to powder rings or any signature of heavily misoriented crystal grains. On the contrary: all diffracting particles are aligned with respect to each other with a maximum angular misfit of some 5°. This observation does not rule out that other clusters of grains with different orientations exist, although we did not succeed in finding any. Random orientations, or even very broad angular distributions of crystalline islands, do not exist in our samples, although Meldrum (personal communication) has reported such a sample from a Sri Lanka locality.

This surprisingly high degree of organization of crystalline grains in an amorphous matrix becomes even more apparent in the full three-dimensional plots of surfaces of equal intensities (Fig. 3). These plots show the weak diffuse scattering intensities around the 200 Bragg reflection. The outer intensity surface is equivalent to 1% of the intensity of the Bragg peak (shown in black inside the cloud of diffuse diffraction). In each figure the view is along the crystallographic $\mathbf{b}$*//$\mathbf{q}_y$ direction. The plots show that for these four samples the diffraction profile is asymmetrically elongated in the $\mathbf{a}$*//$\mathbf{q}_x$ direction with less extension along $\mathbf{c}$*//$\mathbf{q}_z$. The asymmetry relates to the shift of the center of the cloud of diffuse diffraction with respect to the Bragg peak. For $D = 0.1 \cdot 10^{18}$ α-decay events/g the center is shifted toward smaller scattering vectors $\mathbf{q}_x$ while for larger values of D the shift is in the opposite direction. Samples 4605 shows both effects and may well be more heterogeneous than the other samples. For even higher dose levels the diffuse diffraction appears to become more isotropic.

4403   *3104*   *3100*

301   200   004

4304

4105

4103

103

521

004

3107

FIGURE 2. Rocking curves of samples 4403, 3104, 3100, 4304, 4105, 4103, and 3107. Radiation dose is indicated in a/g. The horizontal axis represents the diffraction angle Θ, the vertical axis is the rocking angle ω. Mosaic spread appears as elongation of the rocking signal along the vertical ω axis while particle size and strain also increases the width in the Θ direction.

332

FIGURE 3. Three-dimensional plots of diffuse scattering around the 200 reflection for four samples. The axes are along the reciprocal lattice vectors of the tetragonal zircon structure, the length of the axes is 0.01 1/Å.

DISCUSSION

The mesoscopic nature of metamictization

The results of this study on single crystals with various degrees of radiation damage are in general agreement with earlier results of powder diffraction and transmission electron microscopy investigations (Yada et al. 1981, 1987; Murakami et al. 1991; Weber et al. 1994). These new results allow for the quantification of earlier observations and the discussion of the damage process as a mesoscopic rather than either a macroscopic or atomic-scale phenomenon.

We first compare the excess strain, the macroscopic swelling and particle-size distribution with the idea of a macroscopic phase transition. The nature of the damaged regions in a sample is first analyzed in terms of the relative position of the Bragg reflection and the diffuse halo. In samples with little radiation damage (4403) the halo is shifted to lower diffraction angles with respect to the Bragg reflection. This phenomenon indicates small defect regions with enlarged lat-

tice parameters within the periodic matrix. The local strain is 0.05%, the diameter of the defect regions was estimated using the Scherrer formula for particle-size broadening. This approximation leads to a characteristic diameter of defect regions of some 5 nm in agreement with transition electron microscopic observations (e.g., Yada et al. 1981). The defect regions are well understood as clusters of defects inside a crystalline matrix. The increase of the lattice parameters follows from measurements of powder diffraction patterns (e.g., Murakami et al. 1991) and reaches a maximum of some 7%. No further increase of lattice dimensions was found in this or previous studies (Holland and Gottfried 1955; Weber 1993; Weber et al. 1994).

Low doses of radiation damage lead to a wide mosaic spread (ω-spread) of the single-crystal diffraction pattern. This indicates that various parts of the crystal are twisted against each other. As the mosaic spread correlates with the appearance of local defects, we conclude that the lattice twisting is generated or, at least, enhanced by the local swelling of the defect regions. This idea is also supported by the rapid increase of het-

erogeneous stress broadening in powder diffraction patterns with increasing radiation dose ($D > 4 \cdot 10^{18}$ α decay events/g), and 4×10^{18} is consistent with the results of transmission electron microscopy studies of damage accumulation microtextures (Weber et al. 1994) and the model of damage accumulation proposed by Murakami et al. (1991).

With increasing radiation dose, the single-crystal diffraction pattern changes gradually. At doses smaller than $4 \cdot 10^{18}$ α decay events/g the diffraction angle of the Bragg peak decreases with increasing dose, i.e., the average lattice parameters, a and c, increase with increasing fluence. This increase in unit-cell parameter is consistent with defect accumulation throughout the remaining periodic domains. The position of the Bragg peak is a result of the average defect concentration. The defect concentration can be estimated as follows: each α-particle event may generate ca. 150 defects (Weber 1993). A dose of $2 \cdot 10^{18}$ α decay events/g generates ca. 3×10^{20} Frenkel defects. Per unit cell of ca. $263 \cdot 10^{-24}$ cm³ the equivalent number of defects is 0.36 α decay events/unit cell. The change of lattice volume is 2% for the same defect concentration. The excess volume per defect per unit cell is then 5.5%, which coincides with the upper limit of the observed swelling of the periodic structure for high radiation doses. Here we tacitly assumed that some defects have already recombined with defect concentrations even higher during the early stages of the cascade formation. Furthermore, other defect mechanisms are also relevant, e.g., we expect that the recoil nucleus creates some isolated defects by focused collision cascades. Bearing all these limitations in mind, we conclude that the assumption of a maximum of one Frenkel defect per unit cell is of a reasonable order of magnitude, although the exact nature of these defects remains unclear.

We observed weak, but well-resolved, Bragg peaks even for the highest radiation dose of $7.3 \cdot 10^{18}$ α-decay events/g. Preliminary studies find maxima also in a sample with a dose greater than $10 \cdot 10^{18}$ α-decay events/g. Both samples were previously thought to be fully amorphized and would represent the reference state $\Delta V = 0$ if a "driven" phase transition were to occur. Our experimental results clearly rule out this possibility.

The increase in the average lattice spacing of the crystalline part of the lattice is accompanied by the appearance of diffuse diffraction signals which shift toward larger diffraction angles with respect to the average structure for $D > 0.5 \cdot 10^{18}$ α-decay events/g. This observation indicates that small regions of material with higher densities exist in the sample. The origin of these regions is also not fully understood. Three possible explanations are considered. First, these regions may represent recrystallized, undamaged grains as hypothesized by Holland and Gottfried (1955). Our experimental results show that the relationship between the Bragg peak and the diffuse scattering is similar for all our samples, independent of their geological history. It is hard to understand why the same amount of recrystallization occurs in all samples unless by coincidence (e.g., via similar geological histories of the samples although several samples are from the same occurrence in Sri Lanka (stream gravels in Ratnapura), so that their geologic histories may be similar). The second interpretation was proposed by Murakami et al. (1991). These authors noted that the radiation damage is non-uniform in some of the zircon crystals, that is there are

domains of less and more damaged zircon within the same sample. This feature is clearly present in a zoned zircon (work in preparation). We also observed an extreme tail in the three dimensional diffraction pattern around the 200 reflection in sample 3104, which may well indicate heterogeneous radiation damage. In most other samples used in this study, no significant variation of the diffraction signal was found when the X-ray beam (diameter 0.2 mm) is scanned over the sample surface. Furthermore, the fact that the relative diffraction profiles were essentially sample independent make this mechanism unlikely to be the sole origin of the diffuse scattering. We suggest a third mechanism, which is proposed to always exist, but may coincide with or even be dominated by the previously described mechanisms. This third mechanism is based on the observation that the swelling of the sample via defect accumulation and recoil damage will exert stress on adjacent regions with lower radiation damage (Chakoumakos et al. 1987; Lee and Tromp 1995). Swelling due to recoil damage can reach some 13% in zircon while swelling from localized defects is restricted to ca. 5% with respect to the undamaged material. With a bulk modulus of ca. 200 GPa (Chakoumakos et al. 1991) the local volume stress is equivalent to differential strain of 0.5% (i.e., the maximum shift of the diffuse diffraction cloud with respect to the Bragg peak, e.g., in sample 3107, is equivalent to stress field of the order of 1 GPa). Such stress fields can be absorbed by the sample without systematic fracture and may be reduced by subsequent damage processes. Following this model we expect each crystalline region (with or without localized defects) to be heterogeneously strained by surrounding regions with different doses and degrees of lattice deformation. This heterogeneous strain is then reduced when the crystalline regions become increasingly embedded in an amorphous, heavily damaged matrix in which the local stress is reduced by macroscopic swelling. This has been seen in metamict pyrochlores (Lumpkin and Ewing 1988). The sign of the local stress can even be reversed: a few highly damaged, isolated regions expand and compress the adjacent regions of the sample (i.e., compression of the crystalline material). In more highly damaged material the matrix is expanded while less damaged material now forms islands with lower specific volume than the matrix. In this case the stress at the interface expands the crystalline material and the direction of the stress field is reversed. A typical example with both compression and dilatation appears to be the sample 4605 (Fig. 2), which shows diffuse diffraction signals both for low and high 2θ values.

Note that the densified part of the structure as seen in these experiments still has the zircon structure. The effect has nothing to do with the observation that highly defective zircon may decompose into silica-rich and zirconia-rich regions. Chemical effects of this nature are clearly important in annealed samples and shed much light on the energetics of vitrification (Navrotsky 1991). Our samples showed no chemical segregation (work in preparation).

In samples with radiation doses greater than ca. $4 \cdot 10^{18}$ α decay events/g, the heterogeneous strain becomes less important to the diffraction signal than the particle-size broadening. These samples contain small particles of crystalline material with lattice parameters, which are expanded by the maximum

value of $e_{max} = 4\%$ and characteristic sizes of 5 nm (also see Weber et al. 1994). Increasing radiation dose leads to a decrease in the number of crystalline islands but not to changes of lattice parameters or significant changes of the size of these islands. In contrast to the model of Murakami et al. (1991), we observe only a modest increase of twisting of the orientation of these islands with respect to each other when the radiation dose is increased. The spread of the ω broadening is generally less than $10°$, which indicates that the remaining crystalline islands are still relatively well aligned with respect to each other. Such alignment is still observed in samples with doses of 6.7×10^{18} α-decay events/g and 7.2×10^{18} a-decay events/g. The lack of rotation of the lattice planes shows that the stress fields from the damaged matrix are essentially isotropic and/or that the island appears to have compact shapes such as small spheres. The diffuse scattering is also very isotropic, which excludes the possibility that the crystalline islands form thin plates or needles with fixed crystallographic orientations with respect to the original, undamaged crystal structure.

The weak ω-spread of the Bragg reflections need not exclude the existence of other groups of crystalline islands with different orientations. These other groups were not seen in the diffraction experiment, but no attempts were made to identify all diffraction maxima with similar diffraction angles. Our results clearly show that the angular spread of the diffracting particles, observed in a well-defined part of diffraction space, is surprisingly small.

Does a phase transition occur?

The experimental results indicate that no convergent phase transition or DPT can be deduced either from the macroscopic swelling behavior or from the atomic displacement patterns as seen in the changes of the lattice parameters and the orientation of the crystallographic lattices of the crystalline parts of a sample. A mechanism akin to a DPT does exist on a mesoscopic scale, however. The order parameter of this transition is related to the periodicity of the crystalline structure and can be measured via the pair correlation of structurally equivalent atomic positions. Only short-range order exists in the aperiodic material (the reference state). In radiation damaged material with crystalline islands, the value of the correlation function is larger for small distances than the aperiodic regime and decays sharply for distances larger than the island diameter. Its volume contribution increases with decreasing radiation dose because more crystalline islands exist. Following the tradition of research in the field of structural phase transitions, we now describe the phase transformations starting from the amorphous state as the reference phase (the amorphous state is the fully "symmetry broken" state, i.e., the low-symmetry phase). The control parameter is the radiation dose (starting from infinitely high dose and reducing the dose) or the inverse dose $1/D$ (starting from zero and increasing the inverse dose). In either case, for decreasing radiation doses the size of the crystalline islands increases, they interconnect and finally the entire sample becomes fully crystalline. The transition occurs in the two regimes where either damaged islands exist in the crystalline matrix at low radiation doses or, for high radiation doses, when equivalent crystalline islands exist in an aperiodic matrix. In these two regimes, the order parameter be-

comes proportional to the number of islands per unit volume because our results show that the size of the islands is similar for all islands. The mesoscopic nature of the transition follows now from the observation that radiation events either generate or destroy such islands. For finite volume segments, the mesoscopic order parameter measures the number of islands, whereas the (inverse) radiation dose assumes the role of the control parameter. The transition is now related to the percolation of either the crystalline or the amorphous part of the sample. At the percolation point the minority state ceases to be "islands in a matrix"
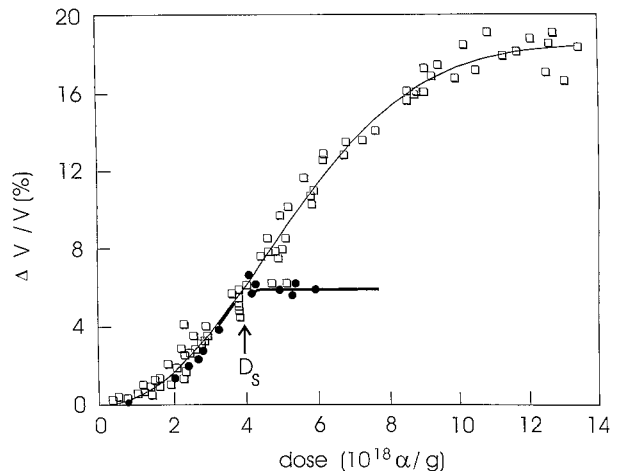

FIGURE 4. Macroscopic swelling (open squares) and unit-cell swelling (filled circles) as a function of fluence (after Weber et al. 1994). The characteristic saturation dose, D_s, is reached when the macroscopic swelling is identical to the saturation swelling of the crystallographic unit cell.
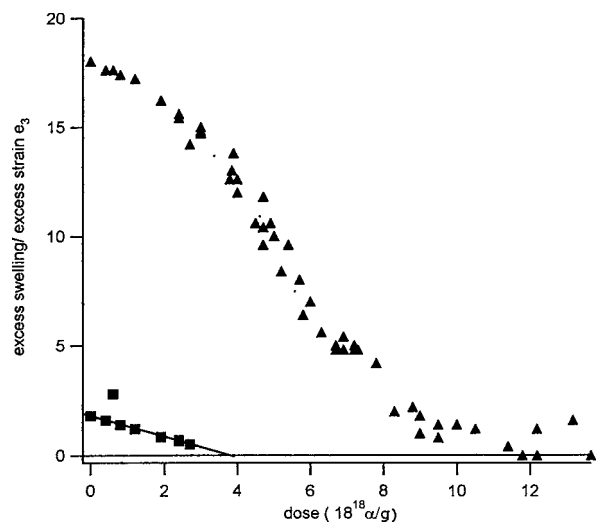

FIGURE 5. Excess volume and excess strains in zircon (after Weber et al.1994). The percolation point is close to the point of disappearance of the spontaneous strain e_3.

but forms an interconnected matrix themselves. The percolation transition (or, more precisely, two percolation transitions for the crystalline and amorphous part, respectively) is, thus, postulated for zircon.

The detailed nature of the percolation transition is difficult to assess from the existing experimental data. Ideally, transport experiments or suitable scattering experiments could help to identify the exact percolation point. In the absence of such experimental results, we can formulate an easily accessible parameter that captures some of the general features of the transition behavior. This parameter is derived from the observation that for low radiation doses the macroscopic expansion and the lattice expansion in the crystallographic c-direction show almost the same dose dependence. In this regime the crystalline matrix is essentially fully connected with embedded isolated amorphous islands. The crystalline matrix is also damaged and contains defects that lead to an expansion of the crystallographic unit cell. At higher doses the damage inside the crystalline parts reaches saturation while the reduction of the crystalline fraction, f_c, leads to further macroscopic swelling. This case has been modeled by Weber et al. (1994, Fig. 5). We can extrapolate the saturation value of the unit-cell expansion, $\Delta V_c/V_c$, to lower doses and determine the dose, D_s, at which the macroscopic swelling has the same value as the saturation cell expansion:

$$\Delta V_m/V_m = (\Delta V_c/V_c)_s \tag{11}$$

The construction in Figure 4 shows that at this dose $D_s = 3.5 \cdot 10^{18}$ α/g for zircon. The excess strain, e_3 (i.e., the strain relative to the saturation value), appears to disappear (Fig. 5) although the exact functional form of the dose dependence of e_3 cannot be determined from the available experimental data. For this reason, we propose the empirical definition for the determination of D_s rather than a critical dose for the disappearance of the excess strain e_3. We anticipate that D_s captures the essential dose dependence of the percolation behavior. Furthermore D_s is easy to measure and can be used in an empirical manner for the comparison of damage generation in different materials (e.g., Ewing et al. 1996).

In summary we find that a phase transition, or, indeed, two phase transitions exist. These are not the traditionally expected "amorphization" transition or the DPT as anticipated in alloys. The phase transitions are related to the percolation of amorphous material in a crystalline matrix and the percolation of crystalline material in an amorphous matrix. The exact percolation behavior remains unknown.

ACKNOWLEDGMENT

REFERENCES CITED

Carpenter, M.A. and Salje, E.K.H. (1994a) Thermodynamics of non-convergent cation ordering in minerals, II: spinels and the orthopyroxene solid solution. American Mineralogist, 79, 1068–1083.
——(1994b) Thermodynamics of non-convergent cation ordering in minerals, III: order parameter coupling in potassium feldspar. American Mineralogist, 79, 1084–1098.
Chakoumakos, B.C., Murakami, T., Lumpkin, G.R., and Ewing, R. (1987) Alpha-decay-induced fracturing in zircon: the transition from the crystalline to the metamict state. Science, 236, 1556–1559.
Chakoumakos, B.C., Oliver, W.C., Lumpkin, G.R., and Ewing, R.C. (1991) Hardness and elastic modulus of zircon as a function of heavy-particle irradiation dose: 1. in situ a-decay event damage. Radiation Effects and Defects in Solids, 40, 118, 393–403.
Chrosch, J. and Salje, E.K.H. (1996) High Resolution X-ray Diffraction methods for the structural characterization of crystalline materials. Ferroelectrics, 187, 1–10.
Degueldre, C. and Paratte, J.M. (1998) Basic properties of a zirconia-based fuel material for light water reactors. Nuclear Technology, 123(1), 21–29.
Ellsworth, S., Navrotsky, A., and Ewing, R.C. (1994) Energetics of radiation-damage in natural zircon (ZrSiO₄). Physics and Chemistry of Minerals, 21, 140–149.
Ewing, R.C. (1994) The metamict state: 1993—The Centennial. Nuclear Instruments and Methods in Physics Research, B91, 22–29.
Ewing, R.C., Chakoumakos, B.C., Lumpkin, G.R., and Murakami, T. (1987) The metamict state. Material Research Society Bulletin, 12, 58–66.
Ewing, R.C., Weber, W.J., and Clinard, F.W. (1995) Radiation effects in nuclear waste forms for high-level radioactive waste. Progress in nuclear energy, 29, 63–127.
Fecht, H.J. and Johnson W.L. (1988) Entropy and enthalpy catastrophe as a stability limit for crystalline material. Nature, 334, 50–51.
Gibbons, J.F. (1972) Ion implantation in semiconductors: Damage production and annealing. Proceedings Institute of Electrical and Electronics Engineers (PIEEE), 60, 1062–1067.
Gong, W.L., Wang, L.M., Ewing, R.C., and Fei, Y. (1996a) Surface and grain-boundary amorphization: Thermodynamic melting of coesite below the glass transition temperature. Physical Review B, 53, 2155–2158.
Gong, W.L., Wang, L.M., Ewing, R.C., and Zhang, J. (1996b) Electron-irradiation- and ion-beam-induced amorphization of coesite. Physical Review, 54, 3800–3808.
Holland, H.D. and Gottfried, D. (1955) The effect of nuclear radiation on the structure of zircon. Acta Crystallographica, 8, 291–300.
Johnson, W.L. (1988) Crystal-to-glass transformation in metallic materials. Materials Science and Engineering, 97, 1–13.
Lam, Nghi Q. and Okamoto, P.R. (1994a) Generalized melting criterion for beam-induced amorphization. Surface and Coatings Technology, 65, 7–14.
——(1994b) A unified approach to solid-state amorphization and melting. Materials Research Society Bulletin, July, 41–46.
Lee, J.K.W. and Tromp, J. (1995) Self-induced fracture generation in zircon. Journal of Geophysical Research, 100(B9), 17, 753–17,770.
Locherer, K.R., Hayward, S., Hirst, P., Chrosch, J., Yeadon, M., Abell, J.S., and Salje, E.K.H. (1996) X-ray analysis of mesoscopic twin structures Philosophical Transactions, Royal Society, London, A 354, p. 2815–2845.
Locherer, K.R., Chrosch, J., and Salje, E.K.H. (1999) Diffuse X-ray Scattering in WO₃. Phase Transitions, in press.
Lumpkin, G.R. and Ewing, R.C. (1988) Alpha-decay damage in minerals of the pyrochlore group. Physics and Chemistry of Minerals, 16, 2–20.
Martin, G. and Bellon, P. (1997) Driven Alloys. Solid State Physics, 50, 189–331.
Meldrum, A., Boatner, L.A., and Ewing, R.C. (1997) Displacive radiation effects in the monazite- and zircon-structure orthophosphates. Physical Review B, 57, 13,805–13,814.
Meldrum, A., Zinkle, S.J., Boatner, L.A., and Ewing, R.C. (1998) A transient liquid-like phase in the displacement cascades of zircon, hafnon and thorite. Nature, 395, 56–58.
Motta, A.T. (1997) Amorphization of intermetallic compounds under irradiation—A review. Journal of Nuclear Materials, 244, 227–250.
Motta, A.T. and Olander, D.R. (1990) Theory of electron-irradiation-induced amorphization. Acta Materialia, 38, 2175–2185.
Murakami, T., Chakoumakos, B.C., Ewing,R.C., Lumpkin, G.R., and Weber, W.J. (1991) Alpha-decay damage in zircon. American Mineralogist, 76, 1510–1532.
Navrotsky, A. (1991) Structure and Energetics of Vitreous and Crystalline Tectosilicates. D Transactions, American Crystallographic Association, 27, 1–12.
Okamoto, P.R. and Meshii, M. (1990) Solid-state amorphization-particle irradiation. In H. Wiedersick and M. Meshii, Eds., Science of Advanced Materials, p. 33–98. American Society for Metals, Metals Park, Ohio.
Salje, E.K.H. (1993) Phase transitions in ferroelastic and co-elastic crystals. Cambridge University Press, Cambridge, U.K.
——(1995) A novel 7-circle diffractometer for the rapid analysis of extended defects in thin films, single crystals and ceramics. Phase Transitions, 55, 37–56.
Salje, E.K.H., Graeme-Barber, A., Carpenter, M.A., and Bismayer, U. (1993) Lattice Parameters, Spontaneous Strain and Phase Transitions in Pb₃(PO₄)₂. Acta Crystallographica, B49, 387–392.
Tsatskis, I. and Salje, E.K.H. (1998) Short range order in a steady state of irradiated Cu-Pd alloys: Comparison with fluctuations at thermal equilibrium. Journal Physics: Condensed Matter, 10, 3791–3806.
Wagner, C. (1952) Thermodynamics in Alloys. Addison-Wesley Publishers, Reading, U.K.
Wang, L.M. and Ewing, R.C. (1992) Ion beam induced amorphization of complex ceramic materials—minerals. Materials Research Society Bulletin, XVII, 38–44.

Wang, L.M. and Weber, W.J. (1998) Transmission electron microscopy study of ion-beam-induced amorphization of $Ca_2La_8(SiOr)_6O_2$. Philosophical Magazine A, in press.

Wang, S.X., Wang, L.M., Ewing, R.C., and Doremus, R.H. (1998a) Ion beam-induced amorphization in MgO-Al_2O_3-SiO_2: I—Experimental and theoretical basis. Journal of Non-Crystalline Solids, 238, 198–213.

———(1998b) Ion beam-induced amorphization in MgO-Al_2O_3-SiO_2: II—Empirical model. Journal of Non-Crystalline Solids, 238, 214–224.

Weber, W.J. (1993) Alpha-decay-induced amorphization in complex silicate structures. Journal of American Ceramic Society, 76, 1729–1738.

Weber, W.J., Ewing, R.C., and Wang, L.M. (1994) The radiation-induced crystalline-to-amorphous transition in zircon. Journal of Materials Research, 9 688–690.

Weber, W.J., Ewing, R.C., Catlow, C.R.A., Diaz de la Rubia, T., Hobbs, L.W., Kinoshita, C., Matzke, H.J., Motta, A.T., Tastasi, M., Salje, E.K.H., Vance, E.R., and Zinkle, S.J. (1998) Radiation effects in crystalline ceramics for the immobilization of high-level nuclear waste and plutonium. Journal of Materials Research, 13, 1434–1484.

Wolf, D., Okamoto, P.R., Yip, S., Lutsko, J.F., and Kluge, M. (1990) Thermodynamic parallels between solid-state amorphization and melting. Journal of Materials Research, 5, 286–301.

Yada, K., Tanji, T., and Sunagawa, I. (1981) Application of lattice imagery to radiation damage investigation in natural zircon. Physics and Chemistry of Minerals, 7, 47–52.

———(1987) Radiation induced lattice defects in natural zircon ($ZrSiO_4$) observed at atomic resolution. Physics and Chemistry of Minerals, 14, 197–204.